PROJECT BIGBIRD XL
COMMERCIAL USE OF THE BENDING/TORSIONAL DRIVE

W. Send, ANIPROP GbR
Sandersbeek 20, D-37085 Göttingen

Summary

The concept for the BigBird XL unmanned aerial vehicle is presented, whose propulsion follows the flapping flight in nature. The technical implementation, called bending/torsional propulsion, allows the functional integration of the two essential features of carrying weight and generating thrust in the wings of the aerial vehicle, which is planned for commercial use. These design features result in virtually silent and highly efficient locomotion. Both aspects justify the expected commercial success. With a wingspan of 5 m, BigBird XL is designed for a take-off weight of up to 25 kg and a payload of up to 10 kg. The design of the aerial vehicle follows from the specification of the primary parameters of degree of evolution, weight and aspect ratio, from which the secondary parameters of wing loading, wing area and wingspan follow directly.

1. INTRODUCTION

The term bending/torsional drive, abbreviated to CBT, refers to the generation of thrust for aircraft with oscillating wings. In the simplified case of a 2D section through a wing, thrust is already generated by the coupled plunging and pitching motion of this inherently rigid wing section.

Added remark: In English-language publications by the author, the term Coupled Bending/Torsional Drive (CBT Drive) has been proposed.

According to this principle, flight devices, starting with the so-called *micro-air-vehicles* via flying creatures and their artificial replicas up to the large dimensions of a man-carrying airplane, generate their thrust preferably with wings mounted on one side. This 3D kinematics of a spatial bending with equal time torsion is accompanied by large deflections of the wings and

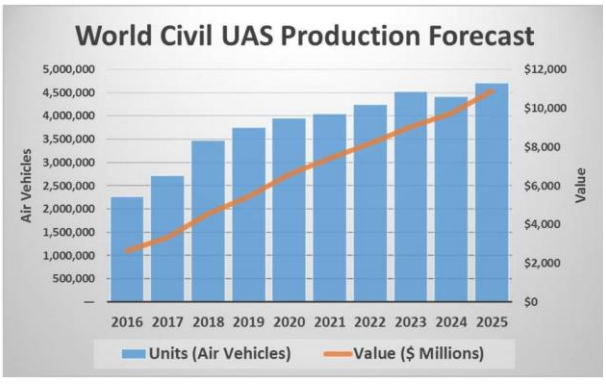

Figure 2: Market development for civil unmanned aerial vehicles according to analyses by the *Teal Group* [1].

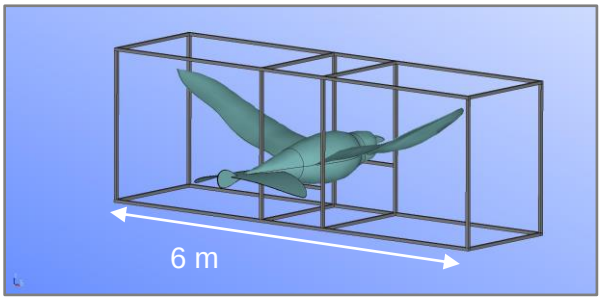

Figure 1. Test stand for BigBird XL. The picture shows the dimensions with a scaled SmartBird.

thus leads both the theoretical prediction and the measurement of the thrust force to limits that have not been overcome so far.

Against this background, the development of a commercial aircraft with CBT for the *Unmanned Aircraft Systems* (UAS) market is a particular economic risk. This risk is justified by the expected benefits in the unmanned aircraft market, which is populated in the size range of BigBird XL (Figure 1) with a wide variety of concepts (see last chapter). The market for this group of aircraft has been booming for several years (Figure 2). The functional integration of the two essential features carrying weight and generating thrust in the wings of the planned aircraft results in virtually silent and highly efficient locomotion. Both aspects are the basis for the expected economic success, since the high efficiency of the CBT, especially compared with multicopters, is directly reflected in significantly longer flight times and greater ranges. The sales expectations are also

based on the spectrum of applications, with agriculture and the energy sector occupying a growing area. Figure 3 shows an example of the US commercial market. *Government* covers areas such as security, surveillance and disaster management, but also research and especially environmental studies.

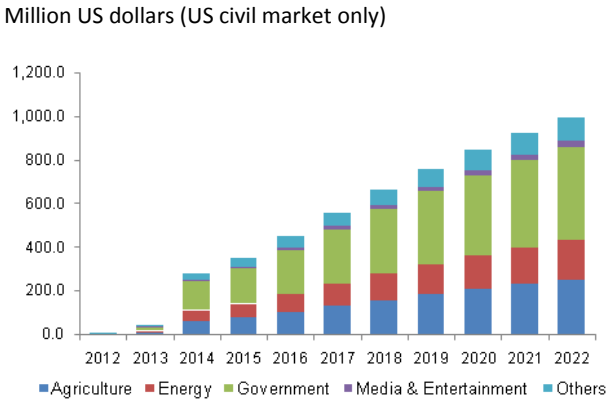

Figure 3. Spectrum of applications for UAS according to analyses by *Grand View Research* [2].

The two graphs cannot prove much more than the dynamics of this market. A more detailed analysis must look at the shares of the various UAV (Unmanned Aerial Vehicle) systems. According to *Grand View Research,* these are divided into

- *Fixed wing UAVs* with rigid wings,
- *Rotary blade UAVs* with one or more rotors, in the latter case the multicopters,
- *Nano UAVs* with the different forms of propulsion, even with simple CBT, and
- *Hybrid UAVs* equipped with various energy sources such as solar panels.

The CBT is found in simple embodiments which all fall among the *nano UAVs*. Depending on the size and range of the UAV, there is now a great deal of competition among the suppliers, but this cannot be discussed further in this paper. After the description of the technical aspects, the paper nevertheless also contains a classification of the system price for BigBird XL at the end, which will be between 100,000 and 150,000 EUR.

The German Federal Ministry for Economic Affairs and Energy (BMWi) has been supporting the project as part of the Central Innovation Programme (ZIM) for SMEs since September 2017 with a two-year grant. The companies involved in the development are those that already developed the artificial bird SmartBird together with Festo AG and presented it at the Hannover Messe in 2011 [3].

The Institute of Flight System Dynamics at RWTH Aachen University has been added as a research partner. For funding reasons, ANIPROP GbR is involved via Steinbeis gGmbH, which is based in Stuttgart, and is responsible for scientific support from design to the accompanying experiments.

2. THRUST GENERATION AND THRUST FORCE: SPECIAL FEATURES OF THE CBT

The measurement of the thrust force of a bending/ torsional drive cannot be considered separately from the aircraft on which this force is generated. In this respect, the CBT differs from all other forms of aircraft propulsion, whose thrust is measured separately on test rigs designed for this purpose. In other words, the CBT is an integral part of the aircraft because it uses the same wings that carry the aircraft. Thus, its mass distribution and the distribution of the reaction force of the surrounding air on the aircraft become determinant parameters of the thrust force actually generated in flight. For the formulation of the flight mechanics of an aircraft with CBT, this is a new level of complication.

The basic mechanism for generating thrust with a coupled 2D plunging and pitching motion or a 3D bending and torsional motion can be regarded as clarified [4]. Therefore, in principle, a theoretical-numerical prediction of the generated thrust force is also possible. This is because the solution of the associated flow problem is based solely on the knowledge of the kinematics of the surface. But the specification of the kinematics must then either start from assumptions or be based on results of a previously measured flight device.

- Because of the large amplitudes, the measurement of the kinematics of a given aircraft with CBT is extraordinarily complicated.
- Experience shows that the high aerodynamic efficiencies achieved in practical flight tests depend very sensitively on the actual phase shift and the amplitude ratio between bending and torsion.

This observation is quite different from computational prediction, which leads to much lower sensitivity depending on the fluid mechanical assumptions.

In principle, the thrust force generated by a CBT only results from the mean value of a periodic motion with large deflections. The oscillating pressure distribution on the wings over the oscillation period is the primary physical parameter (see Fig. 11) and essentially determines the aircraft's performance.

To date, there is no adequate scientific basis for the flight control of such an aircraft.

3. DESIGN OF AN AIRCRAFT WITH CBT

The design of such an aircraft must therefore also break new ground in order to be able to provide realistic specifications for operational flight performance. Such a - more empirical - approach is offered by the *Normal Flyer Diagram* in Figure 4, so called by the author. It can be found in a similar form, among others, also in the beautiful and descriptive book by H. Tennekes [5], where it is called the Large Flight Diagram. The diagram is a "map" of flying creatures as well as aircraft. The diagram shows in full-logarithmic scale on the horizontal axis the weight F_G of an aircraft in the unit Newton, on the vertical axis the wing loading $\gamma = F_G / A$ in N/m². In this, A is the planform area of the wings as defined for fixed wing aircraft in aviation. Arranging the empirical data around a straight line that can be laid across the diagram leads to elementary relationships between these quantities. For this purpose we consider in Figure 5 a cube with edge length *l* and specific weight w (in N/m³).

Assumed an average density for a body, the wing loading increases with the third root of the weight of the body. Now, the flying bodies are not cubes, but flat and elongated bodies with respect to their supporting elements. But even this simple assumption is sufficient for estimating the magnitude

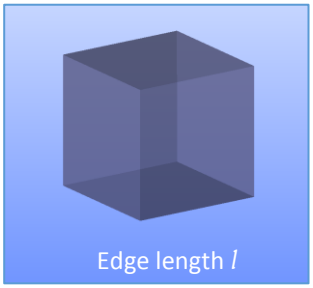

$$G = w \cdot l^3$$

$$A = l^2$$

$$\gamma(G) = \frac{G}{A} = w^{2/3} \cdot G^{1/3}$$

more generally defined

$$\gamma(G) = k_g \cdot \sqrt[3]{G}$$

Figure 5. Elementary relationship between weight G, planform area A and area load. Definition of the degree of evolution k_g .

of k_g . The weight G of such a rectangular wing with $A = l\,b$ amounts to

(1) $$G = g \cdot \rho_K \cdot d \cdot l \cdot b$$

Where g is the gravitational acceleration, ρ_K the mean density of the airfoil, d the thickness, l the wing's chord length and b the span. If we denote the relative airfoil thickness by $\delta = d/l$ and take $\Lambda = b/l$ as the aspect ratio, then after a short conversion for the constant k_g, which is called the *degree of evolution*, we get

(2) $$k_g = [(g \cdot \rho_k \cdot \delta)^2 / \Lambda]^{1/3}$$

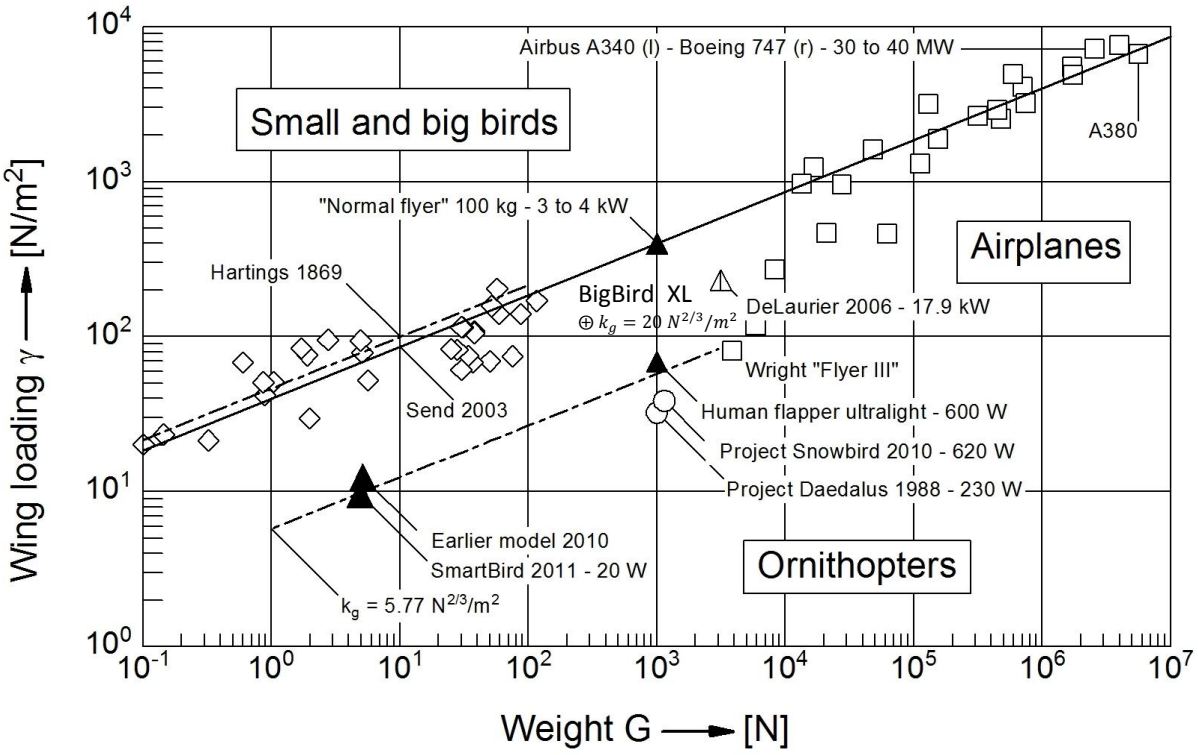

Figure 4. *Normal Flyer Diagram* with the design position ⊕ for BigBird XL, degree of evolution k_g = 20 $N^{2/3}$ /m² and weight force 250 N, corresponding to about 25 kg mass. Associated wing loading = 126 N/m².

The supporting surfaces also include the weight of the fuselage. Assuming 800 kg/m³ for the density of the body (close to "water" for living tissue), 10 m/s² for the acceleration due to gravity, 1/10 for the relative profile thickness and 10 for the aspect ratio leads to the smooth value

(3) $k_g = [(10 \cdot 800 \cdot 0.1)^2/10]^{1/3}$ = 40 N$^{2/3}$ /m^2

which is shown as a solid line in Figure 4. A similar value of 44 N$^{2/3}$/m^2 was already determined at the end of the 19th century by E.J. Marey, who based his figures on P. Harting (for both sources see [6]). The really exciting thing about this line is that the aerial vehicles of the last 20th century have come closer and closer to this line. Starting with the Wright Brothers' *Flyer III,* this "technical evolution of aircraft" ends with the latest large transport aircraft, the *Airbus A380,* at the top right of the diagram.
The keyword *technical evolution* has therefore also been the inspiration for the coefficient in the formula

(4) $$\gamma(G) = \frac{G}{A} =: k_g \cdot \sqrt[3]{G}$$

which is called *degree of evolution* k_g by the author. The formula leads to the following definition of the design of an aircraft with bending/torsional drive, which has been empirically detected:

- An aircraft with CBT is considered fully developed when, at a given weight, it is at or very near the line with the degree of evolution of 40 N$^{2/3}$ /m^2.

Figure 4 shows as an interesting result that the artificial bird *SmartBird* presented by today's developers of the BigBird XL already in 2011 and the *Flyer III of* the Wright brothers have approximately the same degree of evolution. This shows the technical status of the CBT today and the prospects it could have if it is believed to have developed in a similar way to today's jet-powered aircraft.
In this sense, BigBird XL is not designed as a fully developed aircraft. Rather, the degree of evolution has been reduced from the original figure of 25 to the current figure of 20 during the design process. This was done in recognition of the fact that the value of 25 proved to be a too ambitious target in several respects.
The aspect ratio is the third of the three key design parameters for aircraft with CBT:

Weight	G	N
Degree of evolution	k_g	N$^{2/3}$ /m^2
Aspect ratio	Λ	-

The aspect ratio defines the span b via the planform area A known from Equation (4).

(5) $$b = \sqrt{A \cdot \Lambda}$$

With some further assumptions about the load capacity of wings and their drag, which are also valid for other aircraft, these basic data result in the airspeed u_0 and the power requirement P_D.

Lift coefficient 2D	$c_{L,2D}$	-
Correction factor 3D	$k_{3D} = \frac{\Lambda}{\Lambda + 2}$	-
Glide ratio	$\varepsilon = F_L/F_D$	-

The indices L and D are used in accordance with the English terms lift and drag. From the formula for the lift $F_L = |F_G|$

(6) $F_L = k_{3D} \cdot c_{L,2D} \cdot F_0$, with $F_0 = \frac{1}{2} \cdot \rho \cdot u_0^2 \cdot A$

the airspeed u_0 is obtained. The density of the air at 20 °C and 40 % relative humidity is very precisely 1.2 kg/m³. In cruise flight, for which the design is valid, the thrust results in

(7) $$P_D = F_D \cdot u_0 = \frac{F_L}{\varepsilon} \cdot u_0,\ F_T = -F_D$$

By definition, the required thrust F_T in cruise flight must compensate for drag. The glide ratio proves to be a highly speculative quantity with regard to the CBT, where only the execution of the construction provides certainty.
Unlike aircraft with an "external" source of thrust, in the CBT this comes from the moving wings themselves. This is now being investigated.

4. PROCURING THE THRUST POWER

The procurement of the thrust power with CBT for the design of the aircraft is carried out via the unsteady aerodynamics of the coupled plunging and pitching oscillation of the flat plate.

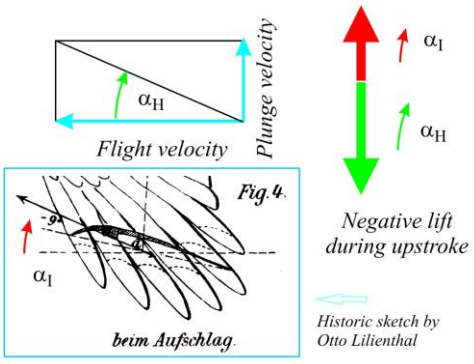

Figure 6. Condition for thrust force with coupled plunging and pitching motion: geometric angle of the pitch smaller than apparent angle of attack of the plunging motion; subsequently $\alpha_{I0} \equiv \alpha_0$.

Here, only the thrust power delivered on average over one oscillation period is of interest. Of course, for the design of the structure, one must know the pressure distribution on the airfoils over the entire oscillation period. The derivation of the formulas for the thrust power is shown in various places. For an understanding of the formulas used in the following, please refer to a simple presentation by the author, which is available on the Internet [7].

Added remark. The preceding reference is a paper written in German. A similar presentation may be found in [7a] in chapter 3 "The Basic Mechanism in 2D Motion".

The condition outlined in Figure 6 for the occurrence of a thrust force with coupled plunging and pitching motion is the physical core of the CBT in the 2D wing section. For the amplitudes h_0 and α_{I0} of the two degrees of freedom at the wing tip this means

$$\frac{\alpha_{H0}}{\alpha_{I0}} > 1, \text{ with } \alpha_{H0} = \frac{h_0 \cdot \omega}{u_0} \quad (8)$$

One can rewrite this condition and replace it by the two dimensionless characteristics *reduced frequency* ω^* and *amplitude ratio* λ.

$$\frac{\alpha_{H0}}{\alpha_{I0}} = \frac{\omega\,(l_m/2)}{u_0} \cdot \frac{h_0}{\alpha_{I0}(l_m/2)} = \omega^* \cdot \lambda \quad (9)$$

In it $\omega = 2\pi f$ with the physical wing beat frequency f. The definitions of ω^* and λ correspond to the formula given above in Equation (9). l_m is the mean chord length with $l_m = A/b$. There is a phase shift κ between plunging and pitching. With the definition on which this is based, the plunge is 90° ahead of the pitch, if the pitch angle (i.e. the geometric angle of attack) reaches its maximum value in the middle between the upper and lower reversal point. At this point, a remark on the role of plunge and pitch should be made.

- The actual thrust power comes from the plunging motion (bending motion in 3D). The amplitude of this degree of freedom remains constant by design. The pitching motion (torsional motion in 3D) converts the power from the plunge into thrust power. It has the role of the "thrust lever" via the amplitude ratio, which is changed by a controllable pitch amplitude. In case the pitch amplitude becomes too large, there is even a thrust reversal possible. The phase shift plays the role of "fine-tuning", in which the conversion of the plunge power into thrust power can still be optimized.

For the design calculation, therefore, only the ratio of the achieved thrust power to the applied plunge power must initially be considered. At this point we should omit the discussion of the extent to which the so-called nose thrust of a wing contributes to the thrust force. The following formulas include only the essential part, which results from the coupling of the two degrees of freedom along the surface of the profile and outside the nose rounding.
This power is defined by the corresponding power coefficient $< c_{\Pi,g} >$ as an average value over one flapping period and is

$$< P_g > = < c_{\Pi,g} > \cdot P_0, \text{ with } P_0 = \frac{1}{2} \cdot \rho \cdot u_0^3 \cdot A \quad (10)$$

The following applies to the applied plunge power

$$< P_h > = < c_{\Pi,h} > \cdot P_0 \quad (11)$$

The two associated power coefficients are simplifications for "small" reduced frequencies

$$< c_{\Pi,g} > = -\pi \cdot (\omega^* \lambda \cdot \sin\kappa - 1) \cdot f_p \cdot \alpha_0^2 \quad (12)$$

$$< c_{\Pi,h} > = \pi \cdot \omega^* \lambda \cdot (\omega^* \lambda - \sin\kappa) \cdot f_p \cdot \alpha_0^2 \quad (13)$$

The form factor f_p reflects that the amplitudes in the respective wing section increase linearly from the wing root to the wing tip and that the chord length also tapers more or less. The assumption "small" refers to the fact that the powers in this case occur simultaneously with the motion without a phase shift caused by trailing vortices. At larger reduced frequencies, there are significant phase shifts between the respective motion and the power it produces in addition to the phase shift between the two degrees of freedom.
The power coefficient $< c_{\Pi,\alpha} >$ for the pitch is numerically small compared to the plunge and can be neglected in the following consideration. Nevertheless, the coefficient plays an essential role for the efficiency of the conversion of plunging power into thrust power later on. The parameter known as *aerodynamic efficiency* η_{aero} indicates what proportion of the power applied at the degrees of freedom of plunging and pitching is converted into thrust.

$$\eta_{aero} = \frac{-< c_{\Pi,g} >}{< c_{\Pi,h} > + < c_{\Pi,\alpha} >} \quad (14)$$

With = 90° and neglecting the pitching power, the aerodynamic efficiency reduces to the simple relation

$$\eta_{aero} \cong \frac{1}{\omega^* \cdot \lambda} \quad (15)$$

Of course, this approximation is only valid if thrust is actually applied by the kinematics of the wings.

- The important step for the design is to specify the aerodynamic efficiency as an <u>estimated value.</u>

This specification must be checked later by recalculation with the full theory and, if necessary,

iteratively readjusted. η_{aero} = 2/3 is a good starting value. As will be explained in more detail below, this means that the effective angle of attack of the wings is about half as large as their geometric angle of attack. The approximate thrust is obtained from

(16) $$< P_g > = -P_D \cong -\pi \cdot \frac{1-\eta_{aero}}{\eta_{aero}} \cdot f_p \cdot \alpha_0^2 \cdot P_0$$

This directly results in the pitch amplitude at the wing tip if the form factor is known.

(17) $$\alpha_0^2 = \frac{|F_G|}{\varepsilon \cdot F_0} \cdot \frac{1}{\pi \cdot f_p} \cdot \frac{\eta_{aero}}{1-\eta_{aero}}$$

For the design, it is sufficient to define a taper μ of the airfoil chord from the wing root l_i to the tip l_a, assumed with the local chord length $l(y)$

(18a) $$\mu := \frac{l_a}{l_i},\ l(y) = l_i(1-(1-\mu)y),\ y \in [0,1]$$

(18b) $$\frac{A}{2} = \frac{b}{2}\int_0^1 l(y) \cdot dy = b \cdot l_i \frac{1+\mu}{4}$$

Since the amplitudes of plunging and pitching should increase linearly from the wing root to the tip, but the reference amplitude α_0 is quadratically included in the power, the form function results in $f(y)$

(19a) $$f(y) = y^2 \cdot l(y),\ y \in [0,1]$$

(19b) $$F_p = \frac{b}{2}\int_0^1 f(y) \cdot dy\,, \quad f_p = \frac{F_p}{A/2}$$

With $l_m = A/b$ follows from Equation (18b) for the chord length at the wing root $l_i = 2l_m/(1+\mu)$. From Equation (19b) it follows for the form factor $f_p = (3\mu+1)/\big(6\cdot(\mu+1)\big)$.

Equation (16) describes the total power. For example, for μ = 0.6 the value f_p = 0.29.

There remains the use of the amplitude α_{H0} of the apparent angle of attack of the plunging motion in Equation (8). It is proportional to the product of plunge amplitude and flapping frequency. By design, the plunge amplitude is the result of the mechanical design of the gearbox. It therefore makes sense to specify this mechanical variable and to check the effect of this on the dynamics of the movement when designing the gear unit.

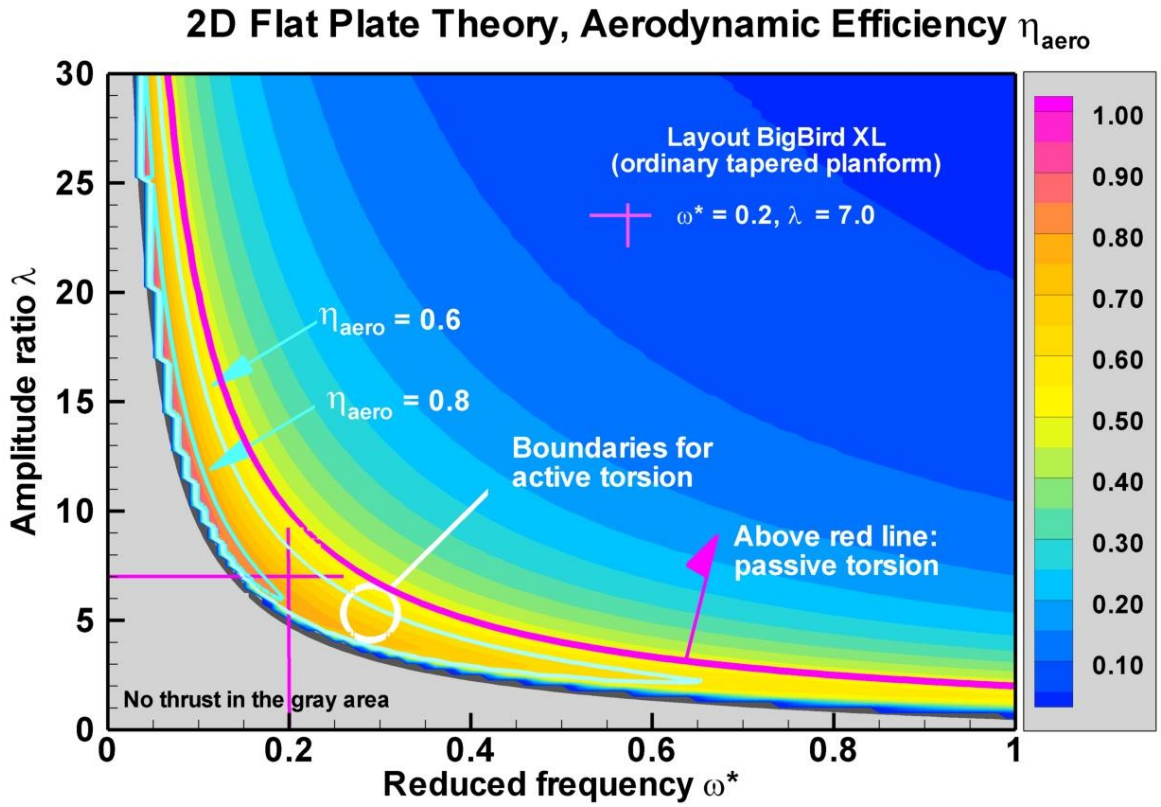

Figure 7. Typical design data for BigBird XL. Mapping of the aerodynamic characteristics to the contour lines for the aerodynamic efficiency from the solution for the oscillating flat plate.

- The dynamics include the flapping frequency itself as well as the effective angle of attack in the individual wing sections. At this angle, the wing sections "see" the incoming flow. The aerodynamic design of the airfoil cross-sections must be able to counteract this incoming flow in such a way that it does not lead to large-scale separation of the flow.

For the amplitude α_{eff0} of the effective angle of attack, according to Equation (8) and Figure 6, the dependency on the aerodynamic efficiency is

$$\alpha_{eff0} = \alpha_{H0} - \alpha_{I0} \cong \frac{1-\eta_{aero}}{\eta_{aero}} \cdot \alpha_{I0} \tag{20}$$

The equation reflects the fact that increasing efficiency leads to smaller and smaller effective angles of attack and consequently to less and less thrust. From Equation (9) follows

$$\alpha_{H0} \cong \frac{\alpha_{I0}}{\eta_{aero}} \cong \frac{h_0 \cdot \omega}{u_0} \tag{21}$$

After the determination of the plunge amplitude h_0 the physical flapping frequency f *is* the last unknown quantity. The aerodynamic parameters *reduced* frequency ω^* and *amplitude ratio* λ can now be used to recalculate the physical quantities. The entry of the values in the diagram with the aerodynamic efficiency from the theory of the oscillating flat plate in Figure 7, together with the other data, gives an initial overview of the flight performance to be expected.

5. EXAMPLE OF LAYOUT

If we take the key data for BigBird XL already given in Figure 4 and add the following values for the other design parameters, then the two essential aerodynamic key figures add up fairly accurately to

reduced frequency ω^* = 0.2 and
amplitude ratio λ = 7.0,

which are entered in Figure 7. However, there is a significant difference from the actual design of the aircraft built at the time as well as the new aircraft.

- The example calculation shown here assumes a simple trapezoidal wing. SmartBird and BigBird XL, on the other hand, have inner and outer wings. The inner wings perform a pure flapping motion, the flapping motion of the outer wings is mechanically amplified by the inner wing.

Such an interpretation is significantly more complicated [8], but at its core it starts with the same data.

Size	Symbol	Value	Unit
Weight	G	250	N
Evolution degree	k_g	20	$N^{2/3}/m^2$
Aspect ratio		10	-
Lift coefficient	$c_{L,2D}$	1.2	-
Glide ratio	ε	10	-
Aerodyn. efficiency	η_{aero}	0.7	-
Em. efficiency 1)	η_{em}	0.8	-
Phase shift	κ	90	deg
Tapering	μ	0.6	-
Plunge amplitude	h_0	0.8	m

1) Electromechanical efficiency

Derived results			
Velocity	u_0	14.5	m/s
Wing area	A	2	m²
Chord length	l_m	0.45	m
Span 2)	$b+r$	5	m
Drag	F_D	25	N
Pitch amplitude	α_{I0}	30	deg
Effective amplitude	α_{eff0}	12.5	deg
Beat frequency	f	2	Hz
Thrust power	P_D	360	W
Drive input power 3)	P_{el}	650	W

2) with fuselage diameter r = 0.55 m

3) nominal from thrust including η_{em} and η_{aero}

Some of the data are rounded up or down slightly. The total power requirement is somewhat greater than P_{el} because active torsion and electronics still have to be added.

6. ASPECTS OF AERODYNAMICS

Three profiles have been investigated so far for the aerodynamic design of the wings, which are shown on the following page. The investigation of the first profile NACA7412 goes back to the time of the development of the predecessors of SmartBird between 2009 and 2011.
For the third profile SG04 exist comprehensive experimental and numerical studies from the Institute of Fluid mechanics at TU Braunschweig [9].
The second profile Eppler e377m is similar to the superimposed wing section 8 of the outer wing of SmartBird, and might also be of interest for BigBird XL. The torsion of the wing is best achieved with the thinnest possible airfoils, with a certain thickness only in the area of the wing spar.
Figure 9 gives an overview of the aerodynamic efficiencies achieved in the range of an amplitude ratio around 7.

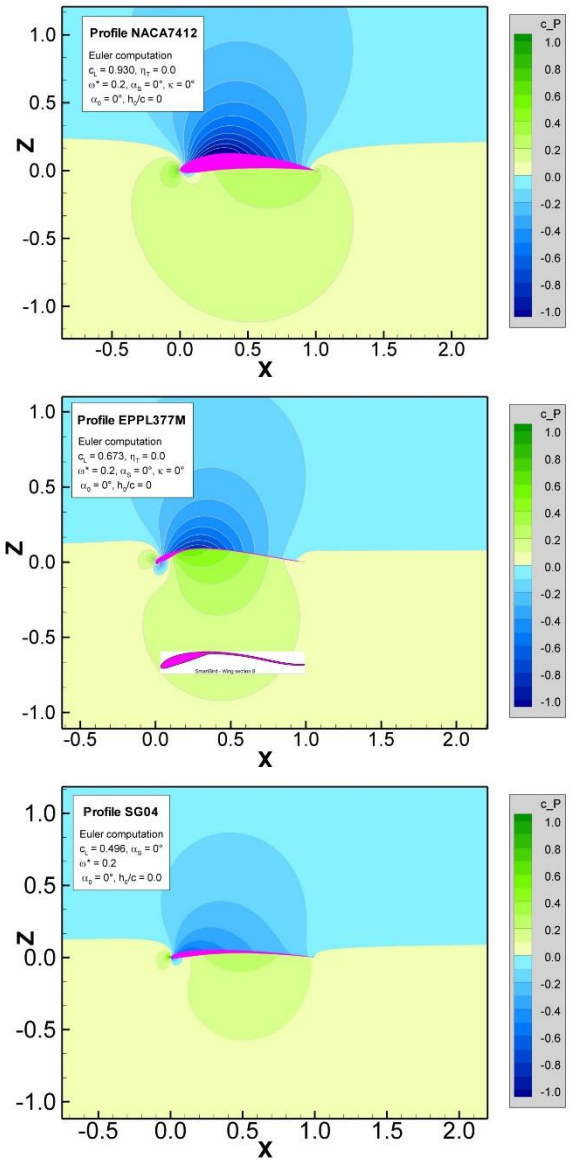

Figure 8. Profiles NACA7412, Eppler e377m and SG04 examined with the software XFOIL and an Euler program for the range Re = 430 000 (based on l_m and u_0).

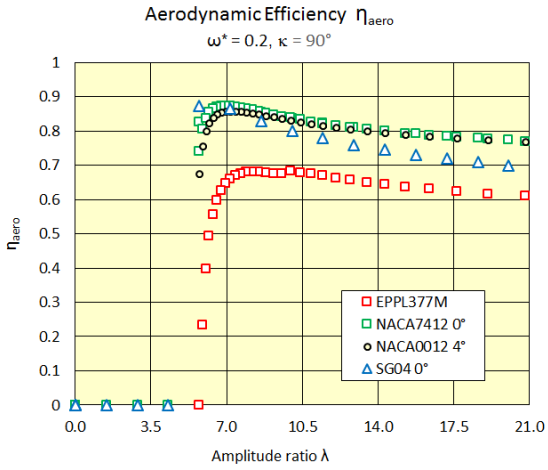

Figure 9. Aerodynamic efficiencies of the selected profiles for the design range.

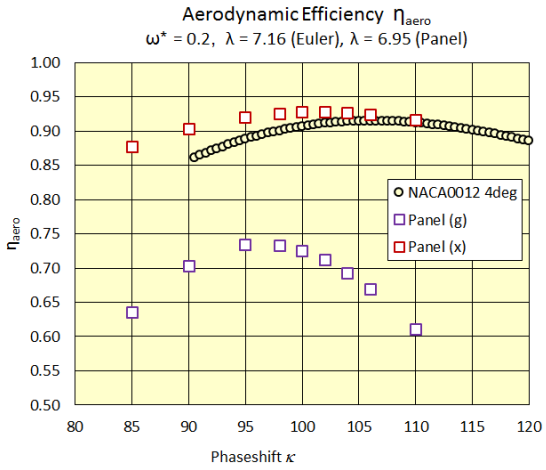

Figure 10. Fine-tuning by changing the phase shift of plunge ahead of pitch. Linear (g) and additionally quadratic (x) components from the computation of the thrust force (Panel) with a panel method.

Even higher efficiencies are achieved by changing the phase angle κ (Fig. 10). For comparison, the profile NACA0012 has also been calculated with a higher order panel method, in which the linear component of the thrust force (pressure distribution along the profile surface) can be calculated separately from the quadratic component (the so-called nose thrust). With the nose thrust - which probably no longer exists at large amplitudes - a significantly higher thrust force and a correspondingly higher efficiency would result. The linear component fits the design calculation in Figure 7. Similar effects also result for the other profiles.
The occurrence of nose thrust in flight at larger amplitudes is a question that has not yet been resolved.

7. RANGE AND CLIMB RATE

The range of an aircraft is determined by the power requirement per kg of flight weight. With the example data of 25 kg and 650 W, this would be a specific power of 26 W/kg, which does not include the power requirement for the active torsion and the on-board system with communication and flight computer. A realistic power requirement of 750 W results in 30 W/kg. This is more efficient than the specific power of 38 W/kg measured for SmartBird. For BigBird XL this results in a power requirement of 750 Wh per hour of flight time in cruise flight. Measured against the mean value of 145 W/kg for multicopters over a wide range of sizes given by G. Strickert [10, Tab. 4], 30 W/kg is a very favorable assumption.

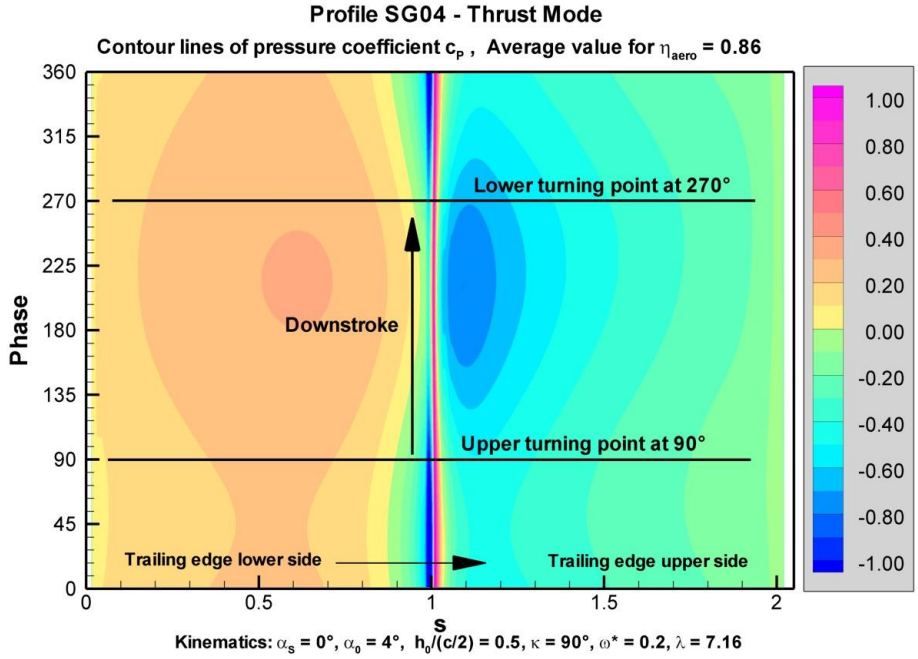

Figure 11. The basis of the load distribution is the analysis of the pressure coefficient over one period. The highest thrust is generated at downstroke fairly close behind the leading edge on the upper side of the airfoil. High efficiency results in a small absolute magnitude of the mean thrust, thus requires an optimal aerodynamic design.

Assuming a weight of up to 10 kg for the batteries carried and a typical specific energy of 150 Wh/kg, 1.5 kWh is available.
Nominally, this is 2 h flight time. The cruising speed of BigBird XL is around 50 km/h. In the available flight time, about 100 km can be achieved, which corresponds to a range of 50 km with outbound and return flight.
The additional power requirement P_C for climbing at the rate of climb u_C results from the lifting power, magnified by the losses due to aerodynamic and electromechanical efficiency.

$$P_C = G \cdot u_C / (\eta_{aero} \cdot \eta_{em}) \quad (22)$$

Using the figures from chapter 5, each 1 m/s results in an additional power of $P_{C,1m}$ = 450 W. In order to reach a height of 10 m 50 m after takeoff, on the basis of u_0 the rate of climb must already be 3 m/s. This nominally requires a drive power of $P_{el,3m}$ = 2 kW. BigBird XL is currently equipped with the brushless motor *Hacker A80-10*, which provides up to 4 kW drive power. The motor together with the controller weighs 1.8 kg.

Remark. A strong e-bike Li-Ion battery (TZI Power, China import) for 48 V and 30 Ah weighs 8.3 kg. Nominally this is 1.4 kWh with a specific energy of 170 Wh/kg. Continuous current may be 30 A, maximum current 55 A. In cruise flight at 750 W, about 15 A flow. Short time, 2.5 kW can be applied. This corresponds to a maximum power density of 300 W/kg.

Propulsion and power supply already account for 10 kg in this case. If the entire remaining structure of the aircraft weighs another 10 kg (which is not yet certain at the time of writing), this leaves a payload of 5 kg.

8. SPECIAL FEATURES AND SYSTEM PRICE

The mission scenario outlined above with a 5 kg payload enables **inspection runs** of 2 h duration with high-quality camera systems, including three-axis stabilization of the camera. This stabilization, known as a *gimbal*, is required because the fuselage of BigBird XL rises and falls by a few centimeters in time with the wing beat. Technically, it is no longer a problem to compensate for this system-related movement.

- In all observation, inspection or surveillance scenarios, BigBird XL's near-silent flight is a major advantage over multicopters.
- The flight time, which is around three to four times longer than that of multicopters due to the lower specific power, considerably increases all types of deployment options.
- In the event of a drive failure with the structure intact, the wings go into a sail position due to the design and without electrics. The aerial vehicle does not fall like a stone from the sky.
- Even if the structure breaks, the aircraft will spin out of the sky uncontrollably, but there are no heavy concentrated masses such as external rotors.
- After all, the appearance of a large bird in the air above areas where people are also present is easier to bear than a drone that is quickly perceived as threatening - even if, objectively speaking, BigBird XL must be assigned to this class of aircraft.

The second major mission scenario is the use as a **cargo UAV** with payloads of up to 10 kg. If we

subtract another 5 kg of weight from the 8.3 kg battery - to stick with the figures mentioned above - then only about 40 % of the original capacity and thus also the range remain. Instead of 100 km flight distance, there are only 40 km left with maximum payload. The range is then 20 km with an outward and return flight. A complex part of the design that has not yet been finalized is the pick-up and set-down of loads. In this area, multicopters or aircraft with swiveling wings (vertical takeoff aircraft) are superior to the propulsion concept of BigBird XL.
Finally, a brief overview should be devoted to the system price, which will be between 100,000 and 150,000 Euros depending on the equipment. In the commercial sector, the following systems stand out:

MAX-8 from XactSense starts at $20,000. The drone comes with a complete camera system, can carry a payload of up to 6.8 kg and flies for up to 35 minutes. The included battery has a capacity of 16 Ah. Titan by XactSense is probably no longer on the market, but was priced at $120,000.

Trimble Gatewing X100 is a small fixed-wing aircraft weighing 2 kg with a wingspan of 1 m, which can remain in the air for up to 45 minutes. It is used especially for surveying tasks. The price is $40,000.

Penguin B UAV is also a fixed-wing aircraft mainly for military purposes with a maximum payload of 10 kg, which can stay in the air for up to 20 hours. The wingspan is 3.3 m. The price starts at about $20,000.

Yamaha R-Max is a Japanese mini helicopter with a 2-stroke combustion engine. The payload is up to 16 kg. The main rotor has a diameter of about 3 m. The aircraft has been on the market for some time and is often used for agricultural purposes. The system price ranges from $150,000 to $230,000 depending on the equipment.

9. OUTLOOK

Challenges for the project that has begun arise in several respects.

- The desired aerodynamic quality with a glide ratio of 12 requires a lightweight, elastic and at the same time pressure-tight covering.
- For the ambitious assumption of 750 W power for horizontal flight, a mechanically efficient transfer of thrust power to the outer wing is required.
- A stiff structure of the wing regarding bending and a soft design for torsion is essential.
- Picking up and setting down loads should be possible without horizontal displacement of the center of gravity.
- The flight control system must meet the requirements of a new type of propulsion concept in which the entire wings are in motion.
- Flight control beyond the line-of-sight horizon must keep the definition of emergency procedures, some of which have not yet been fixed by law.

If BigBird XL meets the expected technical requirements, however, the worldwide flight shows will already be a spectacular event - as has already been shown with SmartBird.

LITERATURE AND SOURCES

[1] Geiger L. *Exclusive Insight: Teal Group's new UAS market report*, UAS Magazine 09/26/2016.

[2] Grand View Research *Commercial UAV Market Size & Analysis Research Report,* Report ID: 978-1-68038-584-7.

[3] Send W, Fischer M, Jebens K, Mugrauer R, Nagarathinam A, Scharstein F. *Artificial Hinged-Wing Bird with Active Torsion and Partially Linear Kinematics*, 28th ICAS Congress, Brisbane, Australia, September 23-28, 2012, paper 53. www.icas.org/ICAS_ARCHIVE/ICAS2012/PAPERS/053.PDF

[4] Send W. Aerofoils *for Bending/Torsional Propulsion - Can We Still Learn from Nature?* Colloquium Luftverkehr an der TU Darmstadt, Vol. 16, ed. Arbeitskreis Luftverkehr der TU Darmstadt 2009. ISBN 978-3-931385-18-7.

[5] Tennekes *H. Hummingbirds and Jumbo Jets*, Birkhäuser Verlag 1997.

[6] Send W. *Winged artifacts*, Ch. 46 in *Living machines - A handbook of research in biomimetics and biohybrid systems*, Oxford University Press 2018.

[7] Send W. *Der Mechanismus des* Schwingenflugs, Annual Meeting DPG Jena1996. www.aniprop.de/sites/default/files/dpg96_vortrag_send.pdf

[7a] Added reference in the English version: www.aniprop.de/sites/default/files/icas06/icas06_send_paper_3.10.4.pdf

[8] Denuder M. *Design and scaling of a bending torsion actuator for coupled impact and torsional vibration*, Master thesis Institute of Fluid Dynamics, ETH Zurich 2014.

[9] Bansmer St. et al. *Experimental and Numerical Fluid-Structure Analysis of Rigid and Flexible Flapping Airfoils,*
AIAA JOURNAL, Vol. 48, No. 9, September 2010.

[10] Strickert G. *Fact check multicopter: similarities and differences to established VTOL configurations*, DLRK 2016, Paper 420026.

■ ■ ■ ■ ■